Nanogrids: A Smart Way to Integrate Public Transportation Electric Vehicles into Smart Grids

Emanuele Ferrandino[a], Antonino Capillo[b],
Fabio Massimo Frattale Mascioli[c] and Antonello Rizzi[d]
Department of Information Engineering, Electronics and Telecommunications, University of Rome "La Sapienza", Via Eudossiana 18, 00184 Rome, Italy

Keywords: Smart Grid, Electric Vehicles, Bidirectional Fast Charge, Renewable Energy Source, Vehicle-to-Grid, Grid-to-Vehicle, Microgrid, Nanogrid, Energy Management System, Fuzzy Logic, Evolutionary Computing, Hierarchical Genetic Algorithm.

Abstract: The need for efficient integration of an Electric Vehicles (EVs) public transportation system into Smart Grids (SGs), has sparked the idea to equip them with Renewable Energy Systems (RESs), in order to reduce their impact on the SG. As a consequence, an EV can be seen as a Nanogrid (NG) whose energy flows are optimized by an Energy Management System (EMS). In this work, an EMS for an electric boat is synthesized by a Fuzzy Inference System-Hierarchical Genetic Algorithm (FIS-HGA). The electric boat follows cyclic routes day by day. Thus, single day training and test sets with a very short time step are chosen, with the aim of reducing the computational cost, without affecting accuracy. A convex optimization algorithm is applied for benchmark tests. Results show that the EMS succesfully performs the EV energy flows optimization. It is remarkable that the EMS achieves good performances when tested on different days than the one it has been trained on, further reducing the computational cost.

1 INTRODUCTION

A SG consists of an energy distribution network that allows to optimize energy exchanges between the internal nodes and the main energy distribution network, also considering EVs charging infrastructures and related Charging Stations (CS). The internal nodes of a typical SG include residential buildings, factories and industries, energy production plants (from renewable sources or from fossil fuels) and storage systems (Commission, 2006).

In an advanced SG, the internal nodes would also include a public transportation system made up of one or more fleets of EVs. Recharging energy infrastructures must be orchestrated in real time in order to ensure continuity of service, thus featuring Grid-to-Vehicle (G2V) services. On the other hand, the Vehicle-to-Grid (V2G) paradigm allows to use the storage system of the EV to power external devices or to feed energy back into the SG (Deng et al., 2015).

With the hypothesis that each EV in the fleet is capable of producing renewable energy on board independently, as well as consuming it, they potentially become an active element of the SG with a function similar to that of a Microgrid (MG). In other words, the EV described above can implement the V2G paradigm with a beneficial energy impact on the SG.

The implementation of the V2G and G2V paradigms, i.e. of bidirectional exchanges of energy, together with the independent RES on board the EVs of a fleet, represents an update of the SG, thanks to the introduction of new prosumers (or active consumers) (Deng et al., 2015; Commission, 2007), which can be summarized as: an increase of the storage energy capacity (the energy storage system of each EV can be considered an extension of the main grid energy storage capacity); an increase of the renewable energy generation capacity (Commission, 2006); an expansion of the SG energy distribution network through mobile agents; a potential increase in SG flexibility and resilience at the cost of an increase in the complexity of the SG EMS, or 'tertiary control' (Olivares and al, 2014).

[a] https://orcid.org/0000-0001-6472-6597
[b] https://orcid.org/0000-0002-6360-7737
[c] https://orcid.org/0000-0002-3748-5019
[d] https://orcid.org/0000-0001-8244-0015

Ferrandino, E., Capillo, A., Mascioli, F. and Rizzi, A.
Nanogrids: A Smart Way to Integrate Public Transportation Electric Vehicles into Smart Grids.
DOI: 10.5220/0010110005120520
In *Proceedings of the 12th International Joint Conference on Computational Intelligence (IJCCI 2020)*, pages 512-520
ISBN: 978-989-758-475-6

Up to now these aspects have been addressed in the literature thanks to the integrations of MGs into the SG (Deng et al., 2015; Arefifar et al., 2012), implemented in single houses (Adika and Wang, 2014) or in small residential agglomerations (Kumar et al., 2017; Hijjo et al., 2016). The purpose of this paper is to propose a solution to extend this approach also to EVs. (Mahmud and al, 2020). In the following, we focus on a specific class of EVs that is introduced alongside the term Nanogrid-vehicle (NG-vehicle). This paper deals with energy management optimization of a single NG-vehicle and validate the hypothesis that it is possible to obtain an adequate optimization of energy management for the case study that will be presented and for similar cases even with short but sufficiently dense data sets.

Section 2 illustrates in detail what we mean by NG-vehicle, the network architecture, its EMS and the objective function chosen for the optimization of the energy flows involving the NG-vehicle. Section 3 illustrates the case study chosen to conduct the experiments, the creation of the data set and the formalization of a mathematical model of the NG-vehicle useful for conducting the experiments in a simulation environment (MATLAB). Section 4 illustrates the optimization method chosen to optimize the NG-vehicle EMS, according to the FIS-HGA paradigm. Section 5 reports an alternative optimization method useful for comparison with that is described in section 4 and forming part of the synthesis procedure of an adequate EMS. In section 6 the synthesis procedure is illustrated and in sections 7 and 8 are reported the results of the experimentation and the conclusions, respectively.

2 NANOGRID-VEHICLE: AN ELECTRIC VEHICLE AS A MICROGRID

We want to highlight the similarities and dissimilarities between a MG, the NG-vehicle and a traditional EV. Unlike a traditional EV, the NG-vehicle can produce energy independently and exchange energy from and to the outside. This factor makes the NG-vehicle a grid, which is composed of the four main nodes characteristic of each MG: generation, load, storage and a link with an external grid.

Unlike a MG, the NG-vehicle does not have a permanent link to the external grid. The Stand-Alone configuration of an MG finds correspondence in the NG-vehicle at all times when it is moving. Conversely, while it is stationary and connected to a CS, it is in the corresponding On-Line configuration of an MG. This peculiarity translates, as we will see below, in the fact that the equation of the inner energy balance depends on a binary variable, which represents the working mode (*'0'*: Stand-Alone, *'1'*: On-Line).

The proposed EV is classified as NG, due to its smaller physical and energy dimensions than a MG. The NG-vehicle requires a energy flow management, or 'secondary control' (Olivares and al, 2014; Kumar et al., 2017; Sabzehgar, 2015). The EMS is responsible for deciding how much energy to exchange with the external grid, represented by a Bidirectional Fast Charge Station (BFCS), as well as the energy flow direction in order to meet the following requirements:

- Be consistent with the problem, i.e. there must be no exchange of energy between the NG-vehicle and the SG when the former is not On-Line;
- Ensure the completion of each route, i.e. do not consume all the energy of the storage system before completing the route;
- Keep the storage system close to the Safety Operation Area (SOA) and make sure that each day starts and ends with a good energy level;
- When the NG-vehicle is On-Line, transfer any surplus energy produced by the on board RES to the SG without compromising the storage system.

We assume that any energy request from the SG is immediately available and that the amount of energy to be delivered can always be accepted by the SG, i.e. the storage energy capacity of the SG is assumed infinite. It is also assumed that both the energy generated by on board renewable source system and the energy required by the propulsion system of NG-vehicle are hard to be predicted. For this reason we have chosen to implement the EMS of the NG-vehicle as a FIS (Santis et al., 2013; Leonori et al., 2017; Gaoua et al., 2013; Leonori et al., 2016a; Ansari et al., 2014).

2.1 NG-vehicle Architecture

Figure 1 illustrates the grid architecture of the NG-vehicle including the EMS and the BFCS.
The square nodes (N and S) can exchange bidirectional energy flows, while the circular nodes (G and L) can exchange unidirectional energy flows (in particular G can only produce energy and L can just consume it). Each node is associated with a variable of the type E_k^X which represents the fraction of energy exchanged by node X in the time-slot k that goes from the discrete instant k to the discrete instant $k+1$. It is assumed that the fraction of energy E_k^X evaluated at the discrete instant k is constant during the entire time-slot. It is also assumed that if at the time-slot

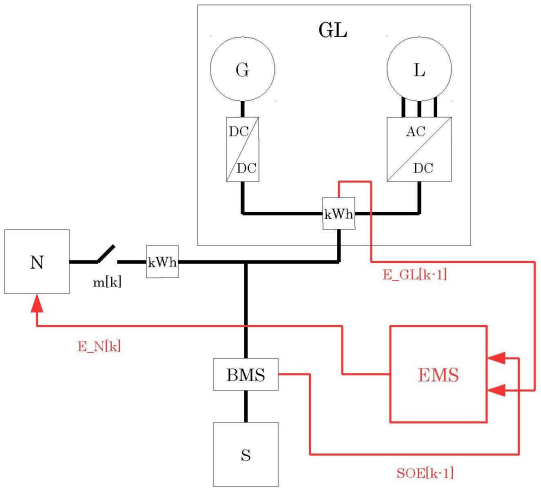

Figure 1: NG-vehicle Architecture and EMS with BFCS link. The EMS, the input variables and the output variable are colored red.

k the node X is producing energy then $E_k^X > 0$, otherwise $E_k^X < 0$. It follows that $E_k^L \leq 0$, $E_k^G \geq 0$ and that E_k^N and E_k^S can be positive, negative or null at any time-slot k.

Aggregating the unidirectional nodes G ad L as a unique bidirectional node allows treating it as a prosumer. So, we will represent with E_k^{GL} the fraction of energy exchanged by GL node. It is possible to readapt the grid architecture of a generic MG to this application (Kumar et al., 2017; Hijjo et al., 2016; Moore and Lopes, 2014; Cheddadi et al., 2015).

In Figure 1 E_{k-1}^{GL} is the fraction of energy measured on the GL node, SOE_{k-1} is the State of Energy measured on the S node and E_k^N is the fraction of energy that controls the N node.

Figure 1 also shows a boolean variable that selects the NG-vehicle mode, m_k, which acts as a gauge of the presence of the link with N. The energy fraction exchanged by S is determined by the energy balance equation (1) and is limited by the actual SOE status and maximum charge/discharge current:

$$E_k^S + E_k^N \times m_k + E^{GL} = 0 \tag{1}$$

$$E_k^S \leq E_k^{S,MaxDischarge} \tag{2}$$

$$E_k^S \geq -E_k^{S,MaxCharge} \tag{3}$$

$$E_k^{S,MaxDischarge} = SOE_k \times E_{max}^S \tag{4}$$

$$E_k^{S,MaxCharge} = (1 - SOE_k) \times E_{max}^S \tag{5}$$

$$E_{max}^S = V_{nom}^S \times I_{max}^S \times dt \tag{6}$$

where V_{nom}^S is the nominal voltage of the storage system, I_{max}^S is the maximum charge/discharge current (determined by the nominal capacity and the maximum C-Rate) and dt is the length of a time-slot expressed in hours (all energy quantities are expressed in kWh).

The SOE is updated through the following formulas:

$$C_k^S = C_{k-1}^S - E_k^S \tag{7}$$

$$SOE_k = \frac{C_k^S}{C_{nom.}^S} \tag{8}$$

where $C_{nom.}^S$ is the nominal capacity of the storage system.

2.2 Objective Function

The objective function is calculated as summation of the NG-vehicle performance for each time-slot of the simulation, for a given EMS. In order to extend the storage system life in terms of charge/discharge cycles, the performance is a measure of the storage stress. The stress of the storage system is due to deep charges and discharges, i.e. charge over 0.8 p.u. and discharge over 0.2 p.u. These values of the SOE define the SOA. Thus, optimization translates into minimizing the objective function. The stress of the storage system is a personalization of the 'penality function' (Leonori et al., 2017; Storti et al., 2015; **?**), illustrated in Figure 2 and whose expression is set out below:

$$P_k^S = f_P(SOE_k) = ((SOE_k - SOE_{opt})/SOE_{opt})^{12} \tag{9}$$

where SOE_{opt} is 0.5 p.u. is the value in which the SOA is centered and in which the penalty function assumes a null value.

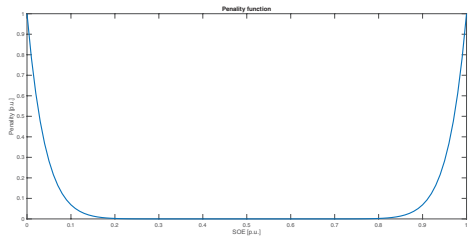

Figure 2: Penality function.

The objective function is calculated as follows:

$$OF = \frac{1}{n} \sum_{k=1}^{n} P_k^S \tag{10}$$

where n represents the length of the experiment in terms of time-slots.

3 CASE STUDY: THE ELECTRIC BOAT VALENTINO III

In the context of the European project Life for Silver Coast - LFSC (LIFE16 ENV/IT/000337), an example of an intermodal sustainable mobility system, our department, in collaboration with the Laboratories of Cisterna di Latina *Polo per la Mobilità Sostenibile* (*POMOS*), are focused on the design and engineering of a small fleet of electric autonomously driven boats dedicated to public transportation and environmental monitoring (Lisena et al., 2016) in inland waters (the Western and Levant Lagoons of Orbetello).

The boats are called Valentino III (see Figure 3), as they represent the third generation of a class of electric trimaran ferry boats. Each boat integrates: an energy generation system based on a photovoltaic plant, which forms the roof, also providing protection to passengers from the sun's rays; an energy storage system based on a battery pack consisting of lithium-ion phosphate cells; a propulsion system, which consists of four paddle wheels independently driven by as many motors located on both the sides of the boat; a BFCS compatible interface.

Figure 3: Rendering of the Valentino III.

Every day the boat must follow four scheduled routes: at 8:00, 10:00, 12:00 and 14:00. The duration of each route is one hour and consists of an outward and a return. For both the lagoons, the piers of Orbetello represent the starting and arrival points of each route, as they are equipped with BFCSs. Both routes cover approximately 6km. This implies that the average speed that the boat must hold is 6km/h or approximately 4kn.

During navigation, the propulsion system must be supplied with adequate power to maintain the speed of navigation and to face winds below ten meters of altitude and surface water currents produced by the wind itself (drift water currents). In addition, the propulsion effort is influenced by the weight on board, which represents mostly passengers and crew members.

3.1 Data Set

A data set was created containing the mooring profiles, photovoltaic generation and consumption of the propulsion system. Project specifications were taken into consideration for the first profile: duration and daily frequency of the routes. For the generation and consumption profiles, it was necessary to obtain in advance the speed profiles of the boat, the use of the public transportation system by people, the photovoltaic generation, winds and surface water currents. With regard to the use of public transportation, it was considered that the weight of the boat has a Gaussian distribution between the dry weight and the fully loaded weight and centered in the middle of the year (high season). An online simulation platform was used for photovoltaic generation and wind data (https://www.renewables.ninja/). The surface water currents profile was created based on the wind profile.

The dynamic equation of motion of the boat was used to calculate the energy consumption data, which uses the speed profile of the boat, the weight profile, the wind profile and the water current profile .

It should be noted that in practice both the energy consumed and the energy produced are unpredictable as it is not known a prior the intensity of the wind and water currents, the number of people on board and the photovoltaic generation.

Finally the data set consists of two sequences $\{(E_k^{GL}, m_k)\}$. Given the cyclical nature of the routes, a time-slot dt equal to 1 minute was chosen, in order to investigate deeply every operational condition of the boat. This results is a very dense data set.

3.2 Adopted Vehicle Model

This section illustrates the formulation of a NG-vehicle model (which also includes a simplifying model of the BFCS). The model is used to simulate the energy flows determined by its EMS and simulation data. The NG-vehicle model also includes the calculation of the objective function which summarizes the performance of the EMS.

The EMS output is the quantity q_k^N defined in the real interval [0,1] which must be translated into the energy fraction E_k^N, as follows:

$$E_k^N = f_N(q_k^N) = E_{max}^N \times (2 \times q_k^N - 1), q_k^N \in [0,1] \quad (11)$$

$$E_{max}^N = P_{nom.}^N \times dt \quad (12)$$

where $P_{nom.}^N$ is the nominal power of the BFCS.

In the same way, the input variable E_k^{GL} is normalized in a quantity $q_k^{GL} \in [0,1]$ defining the inverse model of GL:

$$q_k^{GL} = f_{GL}^{-1}(E_k^{GL}) = \begin{cases} \frac{0.49}{E_{max}^L} \times (E_{max}^L - E_k^{GL}), E_k^{GL} < 0 \\ (E_k^{GL} + E_{max}^G) \times \frac{0.5}{E_{max}^G}, E_k^{GL} \geq 0 \end{cases} \quad (13)$$

$$E_{max}^L = 4 \times P_{nom.}^M \times dt \quad (14)$$

$$E_{max}^G = P_{nom.}^G \times dt \quad (15)$$

where $P_{nom.}^M$ and $P_{nom.}^G$ are the rated powers of each motor and the photovoltaic system, respectively.

The input variable SOE_k on the other hand is already normalized as it is calculated in parts per unit.

4 FIS-HGA DESIGN

EMS synthesis and optimization was carried out by the FIS-HGA paradigm (Santis et al., 2013; Leonori et al., 2017; Siddique and Adeli, 2013; Shi et al., 1999; Capillo et al., 2018; Leonori et al., 2016b), according to which a Mamdani FIS is optimized by a Hierarchical Genetic Algorithm (HGA) (Santis et al., 2017; Delgado et al., 2001; Tang et al., 1998).

4.1 FIS Structure

The FIS consists of two inputs (SOE and E^{GL}) and one output (E^N). The Term Set of each input and of the output counts five Membership Functions (MFs), which partially overlap (Fig. 4).

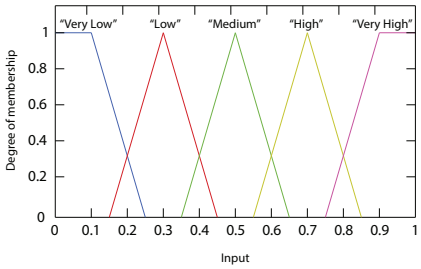

Figure 4: The Term Set for both the two inputs and the output.

The rule base is set to contain all the possible rules (25), which come from the combination between the input MFs, as follows:

$$n_{rules} = n_{MFs}^{n_{inputs}} \quad (16)$$

where n_{rules}, n_{MFs} and n_{inputs} are the numbers of rules, MFs and inputs, respectively. The only logical operator between antecedents is *AND*.

4.2 FIS Genetic Encoding

The FIS is encoded into the genes of the HGA generic individual, as follows:

- The first 10 genes are binary and represent the presence/absence of a MF in the two input Term Sets (not by chance, the size of this set of genes is the product of n_{MFs} by n_{inputs});
- The next 39 genes are real and encode the vertices abscissas of all the input and output MFs. all the abscissas can be tuned, except the ones outside the Universe of Discourse (Fig. 4). The number of these genes is the product of the tunable abscissas of each input and output Term Sets (13) by the total number of inputs and outputs of the FIS (3);
- The next 25 real genes represent the rule weights;
- The last 25 genes are integers selecting MFs from the output Term Sets (each rule must have only one MF in the consequent part).

4.3 The Optimization Process

Two subsequent optimization processes are performed. During the first optimization, the HGA tunes the FIS rule base. Only the first 10 binary genes of the generic individual evolve through generations, while the OF is minimized. If the *i-th* gene is set to 0, this means that the *i-th* MF in the set of the whole inputs MFs (from the first to the last input) is deleted. As a consequence, each rule enclosing the *i-th* MF as antecedent is deleted from the rule set. Thus, the first optimization aims at reducing the number of rules by selecting the most relevant ones for the problem at hand. It is worth mentioning that, when a MF is deleted, the vertices abscissas of the remaining adjacent MFs are modified in order to cover the entire Universe of Discourse (Fig. 5). During the second optimization, the rest of genes of the generic individual evolve over generations, meaning that the FIS parameters (MFs vertices abscissas and rule weights) and the consequent are tuned, while the OF is minimized. Only the genes related to the rule base coming from the first optimization are tuned. In this sense, the first binary genes are at an higher hierarchical level than the others, making the GA hierarchical.

4.4 HGA Operators and Settings

For the first optimization, a one-point crossover is adopted, together with a bit string mutation. For the second optimization, the choice of the crossover operator depends on the type of genes: for the genes of the vertices abscissas, a convex crossover; for the

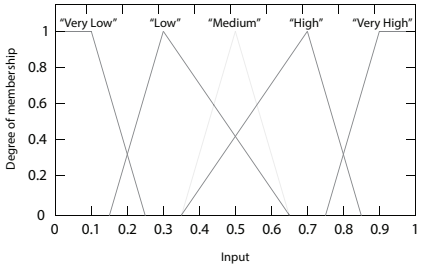

Figure 5: Universe of Discourse coverage after deleting a MF (in this case, the central one).

weights and consequent genes, a uniform crossover. A uniform mutation is performed during the second optimization. A tournament selection with tournament size 2 is chosen for both the first and the second optimization.

The population consists of 100 individuals for both the optimization processes, as well as for the crossover fraction, set to 0.8. The stopping condition is always the reaching of the maximum stall generations while the maximum number of generations is set to 50 for the first optimization and to 300 for the second optimization.

5 CONVEX OPTIMIZATION PROBLEM

In order to know how good is the solution found by optimization through FIS-HGA, it is necessary to find the optimal solution. This can be exactly found by solving a convex optimization problem.

Note that the penalty function expressed in Equation (9) is a convex function of the *SOE*, which is a linear combination of the energy fractions exchanged over time between node N and the NG-vehicle. So the penalty function is a convex function of the EMS output E_k^N, that becomes the variable of the problem.

The problem is a constrained problem. In particular: SOE_k must belong to the real range [0,1]; E_k^S must belong to the real range $[-E_k^{SMaxCharge}, E_k^{SMaxDischarge}]$, in which the extremes depend on the SOE_{k-1}; the fraction of energy E_k^N must belong to the real interval $[-E_{max}^N, E_{max}^N]$.

While it is not even easy to understand whether the problem is convex or not, it is possible in many cases to rewrite a non-convex problem in such a form that it is convex. Some tools can solve optimization problems, even non-convex ones, for example solving the dual problem if it turns out to be convex (Boyd and Vandenberghe, 2004).

The problem can be written as follows:

$$\begin{aligned} &\min_{E_k^N} OF \\ s.t \quad & 0 \leq SOE_k \leq 1 \\ & E_k^S \leq E_k^{SMaxDischarge} \\ & E_k^S \geq -E_k^{SMaxCharge} \\ & \|E_k^N\| \geq \|E_{max}^N\| \\ & E_k^S = -(E_k^N \times m_k + E_k^{GL}) \end{aligned} \tag{17}$$

where OF is described in Equation (10).

6 SYNTHESIS PROCEDURE

The FIS synthesis is the result of the following procedure:

1. Train the FIS by the HGA and solve the convex optimization problem (17) on the Training set; evaluation of the training errors as the Root Mean Square Error Percent - RMSEP on *SOE* and on E^N. If the training errors are too high (greater than 10%) different solutions must be considered:
   - Increase the number of iterations of the HGA;
   - Change the HGA optimization process.
2. Test the HGA optimized FIS and solve the convex optimization problem (17) on sets distinct from the training set; evaluation of the test errors; if the test errors are too high (greater than 10%) it implies data overfitting. It is necessary to repeat steps 1. and 2. until the conditions on RMSEP are met.

The training set is sufficiently rich even lasting only 1 day as a time-slot of 1 minute was chosen, unlike the typical time-slot of 15 minutes, as in (Deng et al., 2015; Olivares and al, 2014; Leonori et al., 2016b; Santis et al., 2017), for data on MGs and SGs. In fact, 1 day contains 1440 samples which is a good amount of data. We are particularly interested in the high season. In particular, for the training set we considered the day in which the highest peak of energy generation by the photovoltaic plant was recorded (indicative of the high season).

7 RESULTS

The significant reduction in the Fuzzy Rule Base, due to the first optimization process (from 25 to 6 Fuzzy Rules), has lead to a lower computational cost for the FIS-EMS synthesis.

The best energy flows returned by the FIS-HGA EMS for the Training Set and the same figures returned by the optimal EMS (optimized by convex optimization), are shown in Figure 6 and Figure 7, respectively. The OF value of the two solutions and the training errors are listed in Table 1.

Table 1: Optimal and SubOptimal OF values, E^N RMSEP (E^N err.) and *SOE* RMSEP (*SOE* err.) on Training day.

Opt.OF p.u.	Sub Opt.OF p.u.	E^N err. %	*SOE* err. %
3.7e-08	5.8e-08	4.56	4.79

It can be seen that for both solutions the requirements of the EMS are met. In particular, in both the solutions, the energy flows between the BFCS and the NG-vehicle show a charging phase of the storage system alternating with each scheduled route to an extent that guarantees the completion of the next route and the containment of the *SOE* in the SOA limiting the stress on the storage system. Furthermore, when recharging does not take place, in the remaining time-windows between two routes, the surplus energy produced by the RES is transferred to the SG, as it is not needed to bring the storage system back to a better *SOE* value.

The EMS optimized by the FIS-HGA performs recharges of the storage system softer and longer than the optimal one. This reduces the time-windows in which the EMS can transfer surplus energy to the SG.

In Figure 8 are shown the E^N RMSEP on the Training day (in the top plot title), the E^N profiles of the two solutions (in the top plot) and the difference between them (in the bottom plot). Figure 9 shows the *SOE* RMSEP (in the top plot title), the *SOE* profiles of the two solutions (in the top plot) and the difference between them (in the bottom plot). Despite the differences in terms of E^N_k, both the RMSEP are lower than the established threshold of 10%, in particular below 5%, allowing to consider the whole synthesis procedure to be effective.

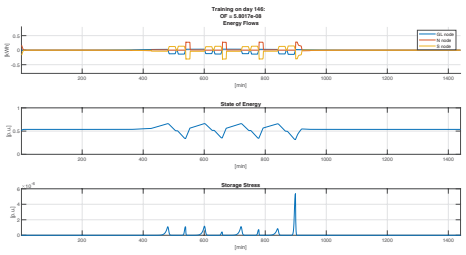

Figure 6: EMS Optimized by FIS-HGA (Training Set).

In order to have a more precise idea of the differences just shown between the EMS optimized by the FIS-HGA and the optimal EMS, the amount of energy

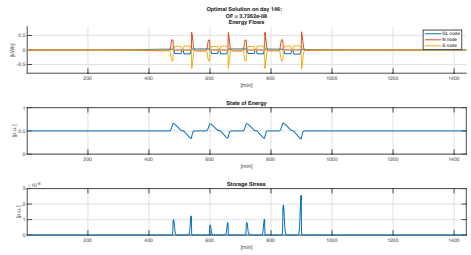

Figure 7: Optimal EMS on Training Set.

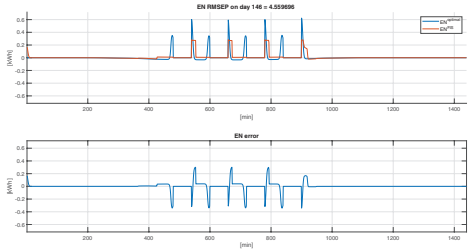

Figure 8: Training error: energy fractions at node N.

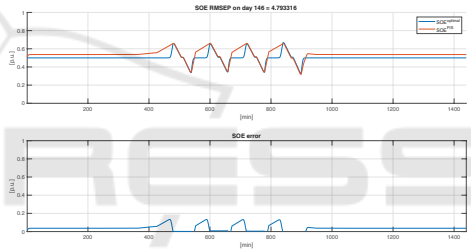

Figure 9: Training error: State of Energy.

taken from the SG in one day, Q^N_{buy}, and the amount of energy transferred to the SG in one day, Q^N_{sell}, for the two solutions are shown in Table 2.

Table 2: Optimal and Sub-Optimal energy from and to the SG.

Q^N_{sell} kWh	Q^N_{buy} kWh	$Opt.Q^N_{sell}$ kWh	$Opt.Q^N_{buy}$ kWh
2.586	17.472	7.374	21.561

Note that the use of NG-vehicles for the implementation of a transportation system has a lower energy impact on the SG of Q^N_{sell}, compared to the use of equivalent EV without RESs (Eq. EVs).

In Table 3 are summarized the results of the test phase performed by simulating the EMS obtimized by FIS-HGA and solving the convex optimization problem (17) for the eight days. The E^N and *SOE* RMSEP values are below the 10% threshold for all tests: the optimization of the EMS through FIS-HGA on the Training Set has generated a solution that is valid throughout most of the year. The worst result is that

Table 3: Optimal and Sub Optimal OF values on Test days, E_k^N RMSEP (E_k^N err.) and *SOE* RMSEP (*SOE* err.) on Test days.

Test day	Opt.OF p.u.	Sub Opt.OF p.u.	E^N err. %	*SOE* err. %
59	9.7e-10	3.0e-09	2.18	4.63
90	1.0e-09	2.5e-07	2.93	6.85
120	1.8e-09	4.4e-08	3.52	5.48
151	6.0e-07	5.3e-04	6.33	8.78
181	8.4e-07	1.4e-05	5.74	5.37
212	1.3e-07	7.9e-07	5.08	4.71
243	2.2e-09	1.1e-07	3.93	5.10
273	1.1e-09	4.2e-08	2.89	5.63

related to the day 151 (high season). This is explained by the fact that around this day the maximum weight at full load is recorded; remember that the weight on board, representing the people who use the transportation service offered by the single boat, strongly influences the consumption of the propulsion system.

8 CONCLUSIONS

The EMS of an NG-Vehicle has been synthesized through a FIS-HGA algorithm, aiming at managing the bidirectional exchanges of energy fractions with an SG through a BFCS according to the time-windows in which the NG-vehicle is On-Line and the completion of the scheduled routes. The EMS optimization was performed aiming to minimize the storage stresses possibly due to deep charges/discharges of the NG-vehicle storage system. The synthesis of EMS as FIS through the proposed procedure has proved effective in avoiding data overfitting. These choices led to a synthesis with a satisfactory performance value for all the 8 test days, as also reported by the RMSEP values. The synthesized EMS has satisfied all the proposed requirements. In particular, the NG-vehicle transfers its energy surplus to SG, due to the continuity of the energy production by the photovoltaic roof. Therefore, since the optimization aims at minimizing the stress on the storage system, the generation system from renewable sources on board not only supports the storage system during Stand-Alone mode (i.e. navigation mode), as commanded by the NG-vehicle architecture, but it reduces the energy impact that the NG-vehicle has on the SG.

Figure 10 shows the energy impacts on the SG of the Valentino III with sub-optimal EMS, the Valentino III with the optimal EMS and the Eq.-EV (Valentino III without RES), for each of the eight test days. Results show that the energy impact of the Valentino III with sub-optimal EMS is closer to the energy impact

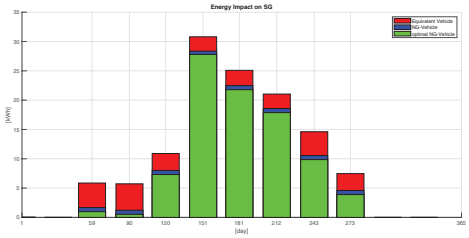

Figure 10: Energy Impact on the SG of the Valentino III Eq-EV, the Valentino III with sub-optimal EMS and the Valentino III with optimal EMS.

of the one with optimal EMS than to the energy impact of the Eq.-EV. Future analisys will be performed in order to increase the difference in terms of energy impact from the worst case. To achieve this goal, one way consists in performing an optimization with the same FIS-HGA algorithm, while minimizing both the stress on the storage system and the energy impact on the SG.

We also reserve for the future the wider topic of optimizing the energy flow management of a fleet of NG-vehicles.

ACKNOWLEDGMENTS

The POMOS Laboratories and the DIET Department (University of Rome “La Sapienza”) would like to thank the EU for financial support to environmental and climate action projects like LIFE for Silver Coast (LIFE16 ENV/IT/000337). Such a help is crucial to achieve natural and historical preservation of Italy, especially of touristic areas.

REFERENCES

Adika, C. and Wang, L. (2014). Autonomous appliance scheduling for household energy management. *IEEE Transactions on Smart Grid, vol. 5, no. 2*, pages 673–682.

Ansari, M., Al-Awami, A., Abido, M., and Sortomme, E. (2014). Optimal charging strategies for unidirectional vehicle-to-grid using fuzzy uncertainties. *IEEE PES TD Conference and Exposition*, pages 1–5.

Arefifar, S., Mohamed, Y., and El-Fouly, T. (2012). Supply-adequacy-based optimal construction of microgrids in smart distribution systems. *IEEE Transactions on Smart Grid, vol. 3, no. 3*, pages 1491–1502.

Boyd, S. and Vandenberghe, L. (2004). *Convex Optimization*. Cambridge University Press.

Capillo, A., Luzi, M., Paschero, M., Rizzi, A., and Mascioli, F. F. (2018). Energy transduction optimization of a wave energy converter by evolutionary algorithms.

International Joint Conference on Neural Networks (IJCNN), pages 1–8.

Cheddadi, Y., Gaga, A., Errahimi, F., and Es-Sbai, N. (2015). Design of an energy management system for an autonomous hybrid micro-grid based on labview ide. *3rd International Renewable and Sustainable Energy Conference (IRSEC)*, pages 1–6.

Commission, E. (2006). *The SmartGrids European Technology Platform — SmartGrids*. Luxembourg.

Commission, E. (2007). *Strategic Research Agenda for Europe's Electricity Networks of the Future*. Brussel.

Delgado, M. R., Zuben, F. V., and Gomide, F. (2001). Hierarchical genetic fuzzy systems. *Information Sciences, Vol.136*, page 29 – 53.

Deng, R., Yang, Z., Chow, M., and Chen, J. (2015). A survey on demand response in smart grids: Mathematical models and approaches. *IEEE Transactions on Industrial Informatics, vol. 11, no. 3*, pages 570–582.

Ehsani, M., Gao, Y., and Emadi, A. (2009). *Modern electric, hybrid electric, and fuel cell vehicles: fundamentals, theory, and design*. CRC Press.

Gaoua, Y., Caux, S., Lopez, P., and Salvany, J. (2013). Online hev energy management using a fuzzy logic. *12th International Conference on Environment and Electrical Engineering, EEEIC*, pages 46–51.

Hijjo, M., Felgner, F., Meiers, J., and Frey, G. (2016). Energy management for islanded buildings integrating renewables and diesel generators. *IEEEPES Power-Africa, Livingstone*, pages 62–66.

Kumar, A., Deng, Y., He, X., Kumar, P., and Bansal, R. (2017). Energy management system controller for a rural microgrid. *The Journal of Engineering, vol. 2017, no. 13*, pages 834–839.

Leonori, S., Paschero, M., Rizzi, A., and Mascioli, F. F. (2016a). Optimization of a microgrid energy management system based on a fuzzy logic controller. *IECON*.

Leonori, S., Paschero, M., Rizzi, A., and Mascioli, F. F. (2017). An optimized microgrid energy management system based on fis-mo-ga paradigm. *Fuzzy Systems (FUZZ-IEEE)*, pages 1–6.

Leonori, S., Santis, E. D., Rizzi, A., and Mascioli, F. F. (2016b). Multi objective optimization of a fuzzy logic controller for energy management in microgrids. *IEEE Congress on Evolutionary Computation (CEC)*, pages 319–326.

Lisena, V., Paschero, M., Gentile, V., Amicucci, P., Rizzi, A., and Mascioli, F. F. (2016). A new method to restore the water quality level through the use of electric boats. *IEEE International Smart Cities Conference (ISC2)*, pages 1–4.

Mahmud, K. and al (2020). Real-time load and ancillary support for a remote island power system using electric boats. *IEEE Transactions on Industrial Informatics, vol. 16, no. 3*, pages 1516–1528.

Moore, R. and Lopes, J. (2014). The energy management and optimized operation of electric vehicles based on microgrid. *IEEE Transactions on Power Delivery, vol. 29, no. 3*, pages 1427–1435.

Olivares, D. and al (2014). Trends in microgrid control. *IEEE Transactions on Smart Grid, vol. 5, no. 4*, pages 1905–1919.

Sabzehgar, R. (2015). A review of ac/dc microgrid-developments, technologies, and challenges. *IEEE Green Energy and Systems Conference (IGESC)*, pages 11–17.

Santis, E. D., Rizzi, A., and Sadeghian, A. (2017). Hierarchical genetic optimization of a fuzzy logic system for energy flows management in microgrids. *Applied Soft Computing, vol. 60*, pages 135 –149.

Santis, E. D., Rizzi, A., Sadeghiany, A., and Mascioli, F. (2013). Genetic optimization of a fuzzy control system for energy flow management in micro-grids. *Joint IFSA World Congress and NAFIPS Annual Meeting (IFSA/NAFIPS)*, pages 418–423.

Shi, Y., Eberhart, R., and Chen, Y. (1999). Implementation of evolutionary fuzzy systems. *IEEE Transactions on Fuzzy Systems, vol. 7, no. 2*, pages 109–119.

Siddique, N. and Adeli, H. (2013). *Computational Intelligence: Synergies of Fuzzy Logic, Neural Networks and Evolutionary Computing*. Wiley.

Storti, G., Paschero, M., Rizzi, A., and Mascioli, F. (2015). Comparison between time-constrained and time-unconstrained optimization for power losses minimization in smart grids using genetic algorithms. *Neurocomputing, vol. 170*, page 353 – 367.

Tang, K., Man, K., Liu, Z., and Kwong, S. (1998). Minimal fuzzy memberships and rules using hierarchical genetic algorithms. *IEE Transactions on Industrial Electronics, vol. 45, no.1*, pages 162–169.